https://doi.org/10.5194/os-2019-107
Preprint. Discussion started: 7 October 2019

Ocean Science
Discussions
Open Access
EGU

Impact of tidal dynamics on diel vertical migration of zooplankton in Hudson Bay

Vladislav Y. Petrusevich[1*], Igor A. Dmitrenko[1], Andrea Niemi[2], Sergey A. Kirillov[1], Christina Michelle Kamula[1], Zou Zou A. Kuzyk[1], David G. Barber[1] and Jens K. Ehn[1]

[1]University of Manitoba, Centre for Earth Observation Science, Winnipeg, Canada
[2]Fisheries and Oceans Canada, Winnipeg, Manitoba, Canada

Correspondence to: Vladislav Y. Petrusevich (vlad.petrusevich@umanitoba.ca)

Abstract. Hudson Bay is a large, seasonally-ice covered Canadian inland sea, connected to the Arctic Ocean and North Atlantic through Foxe Basin and Hudson Strait. This study investigates zooplankton distribution, dynamics and factors controlling them during open water and ice cover periods (from September 2016 to October 2017) in Hudson Bay. A mooring equipped with two Acoustic Doppler Current Profilers (ADCP) and a sediment trap was deployed in September 2016 in Hudson Bay ~190 km north-east from the port of Churchill. The backscatter intensity and vertical velocity time series showed a pattern typical for the zooplankton diel vertical migration (DVM). Zooplankton collected by the sediment trap allowed for the identification of migrating scatters during the study period. From the acquired acoustic data we observed the interaction of DVM with multiple factors including lunar light, tides, as well as water and sea ice dynamics. Solar illuminance was the major factor determining migration pattern, but unlike at some other polar and sub-polar regions, moonlight had a little effect on DVM, while tidal dynamics is important. The presented data constitutes a first-ever observed presence of DVM in Hudson Bay during winter as well as its interaction with the tidal dynamics.

1 Introduction

The synchronized diel vertical migration (DVM) of zooplankton is an important process of the carbon and nitrogen cycle in marine systems, because it effectively acts as a biological pump, transporting carbon and nitrogen vertically below the mixed layer by respiration and excretion (Darnis et al., 2017; Doney and Steinberg, 2013; Falk-Petersen et al., 2008). DVM of zooplankton is a synchronized movement of individuals through the water column and is considered to be the largest daily synchronized migration of biomass in the ocean (Brierley, 2014). This migration is majorly controlled by two biological factors: (1) predator avoidance by staying away from the illuminated surface layer during the day and thus reducing the light-dependent mortality risk (Hays, 2003; Ringelberg, 2010; Torgersen, 2003) and (2) optimization of feeding, with the assumption that algal biomass is greater in the surface layer during evening hours and zooplankton rise to feed on it in the evening (Lampert, 1989). The following research question needs to be addressed: what sets the timing of this synchronized movement in the Arctic environment?

Earlier studies of DVM in the Arctic were focused on the period of midnight sun or the transition period from midnight sun to a day/night cycle (Blachowiak-Samolyk et al., 2006; Cottier et al., 2006; Falk-Petersen et al., 2008; Fortier, 2001; Kosobokova,

https://doi.org/10.5194/os-2019-107
Preprint. Discussion started: 7 October 2019

1978; Rabindranath et al., 2010). Recent studies based on acoustic backscatter data and zooplankton sampling showed the presence of synchronized DVM behavior continuing throughout the Arctic winter, during both open and ice-covered waters (Båtnes et al., 2015; Benoit et al., 2010; Berge et al., 2009, 2012, 2015a, 2015b; Cohen et al., 2015; Last et al., 2016; Petrusevich et al., 2016; Wallace et al., 2010). It was proposed (Berge et al., 2014; Hobbs et al., 2014; Last et al., 2016; Petrusevich et al., 2016) that, during polar night, DVM is regulated by diel variations in solar and lunar illumination, which are at intensities far below the threshold of human perception. Another reason for increasing interest in studying DVM patterns in various geophysical and geographical environments and their seasonal changes in response to changing oceanographic conditions is that they could help to inform us about physical oceanographic processes. Furthermore, DVM pattern can be significantly modified by water column stratification (Berge et al., 2014) and water dynamics, such as polynya induced estuarine-like circulation (Petrusevich et al., 2016), tidal currents (Hill, 1991, 1994; Valle-Levinson et al., 2014), and upwelling/downwelling (Dmitrenko et al., 2019; Wang et al., 2015).

In the Arctic Ocean, the DVM process can be difficult to measure. However, there has been a recent success in using data obtained by an Acoustic Doppler Current Profiler (ADCP), which is a modern oceanographic instrument commonly used to measure the vertical profile of current velocities. Because the velocity profiling by an ADCP is based on processing the measured intensity of acoustic pings backscattered by suspended particles in the water column, further processing of the measured acoustic backscatter to volume backscatter strength (Deines, 1999) has been successful in quantifying zooplankton abundance (Bozzano et al., 2014; Brierley et al., 2006; Cisewski et al., 2010; Cisewski and Strass, 2016; Fielding et al., 2004; Guerra et al., 2019; Hobbs et al., 2018; Last et al., 2016; Lemon et al., 2008; Petrusevich et al., 2016; Potiris et al., 2018, etc.). ADCP backscatter data, validated using a time-series of zooplankton samples collected from sediment traps, provides a particularly useful tool for understanding the effects of physical oceanographic processes on zooplankton DVM, changes in zooplankton community composition throughout the year, and an overall better understanding of the marine ecosystem function and carbon cycling (Berge et al., 2009; Willis et al., 2006, 2008).

In this study, factors controlling zooplankton distribution during the open-water and ice-covered periods are investigated using ADCP data together with sediment trap samples for the first time in Hudson Bay. The main objectives are to (1) examine DVM during open water and ice-covered seasons in Hudson Bay in 2016-2017, (2) identify zooplankton species involved in DVM and (3) describe the DVM response to lunar light, tides, water and sea-ice dynamics.

2. Study Area

Hudson Bay (Figure 1a) is a large (with an area about 831,000 km^2) seasonally ice-covered shallow inland sea with an average depth of 125 m and maximum depth below 300 m (Burt et al., 2016). The seabed is characterized by fluted tills, postglacial infills, moraines and subglacial channels eroded to bedrock resulting in bottom depth varying from two hundred meters to ~10 m (Josenhans and Zevenhuizen, 1990). The tides are mostly lunar semidiurnal (M_2) with an amplitude of about 3m at the entrance to Hudson Bay from Hudson Strait (Prinsenberg and Freeman, 1986; St-Laurent et al., 2008) and about 1.5m in

https://doi.org/10.5194/os-2019-107
Preprint. Discussion started: 7 October 2019

Churchill (Prinsenberg, 1987; Saucier et al., 2004)l (Figure 1) (Ray, 2016). The marine water masses flow into Hudson Bay through two gateways: (1) Gulf of Boothia – Fury and Hecla Strait – Foxe Basin, and (2) the Baffin Bay – Hudson Strait (Fig. 1a). Measurements of alkalinity and nutrient ratios suggest that the water masses within Hudson Bay are dominated by Pacific-origin waters from the Arctic Ocean (Burt et al., 2016; Jones et al., 2003) and the phytoplankton and zooplankton assemblages resemble those in the Arctic Ocean (Estrada et al., 2012). Freshwater inputs to Hudson Bay are very large, including river runoff from the largest watershed in Canada, together with seasonal inputs of sea ice-melt. The freshwater inputs together produce strong stratification at the surface in summer (Ferland et al., 2011). Fall storms and cooling followed by brine rejection from sea ice formation during winter produces a winter surface mixed layer varying from ~40 to >90 m deep throughout Hudson Bay (Prinsenberg, 1987; Saucier et al. 2004).

Hudson Bay is ice-covered during 7–9 months a year with ice formation typically starting in the north-west part of the bay in late October (Hochheim and Barber, 2014). The mean maximum ice thickness ranges from 1.2 m at the north-west to 1.7 m in the east (Landy et al., 2017). Around Churchill, the ice usually starts forming in October-November and breaks up in May-June (Gagnon and Gough, 2005, 2006). Since 1996 the open water season has, on average, increased by 3.1 (±0.6) weeks in Hudson Bay, with mean shifts in dates for freeze-up and break-up of 1.6 (±0.3) and 1.5 (±0.4) weeks accordingly (Hochheim and Barber, 2014).

There have been few studies of zooplankton community composition in Hudson Bay. Among the microzooplankton species found in Hudson Bay, *Sagitta elegans* is the most abundant species, followed by *Aglantha digitale* as the second most abundant (Estrada et al., 2012). The mesoplankton community in Hudson Bay is dominated by small copepods*: Oithona similis, Oncaea borealis*, and *Microcalanus* (Estrada et al., 2012). Zooplankton diversity is generally low at high latitudes (Conover and Huntley, 1991). Typically, salinity gradients and freshwater discharge play an important role in determining species diversity (Witman et al., 2008). Seasonality in food availability is another significant challenging factor for zooplankton in high latitudes (Bandara et al., 2016; Carmack and Wassmann, 2006; Varpe, 2012).

3. Data Collection and Methods

3.1 Mooring Configuration and Set up

A bottom-anchored oceanographic mooring (Fig. 1b) was deployed at 109 m depth ~190 km north-east from the port of Churchill (59° 58.156’ N 91° 57.144’ W) 26 September 2016 and recovered on 30 October 2017. The mooring setup consisted of (i) one upward-looking 5-beam Signature 500 ADCP by Nortek placed at 38 m depth, (ii) upward-looking 4-beam 300 kHz Workhorse Sentinel ADCP by RD Instruments placed at 106 m depth and (iii) one Gurney Instrument “Baker Type” sequential sediment trap (Baker and Milburn, 1983) at 85 m with collection area of 0.032 m^2. Several conductivity-temperature, conductivity-temperature-turbidity and temperature-turbidity sensors were also deployed at various depths on the mooring, but the data obtained by these sensors were not analyzed in this study.

https://doi.org/10.5194/os-2019-107
Preprint. Discussion started: 7 October 2019

The velocity and acoustic backscatter (ABS) intensity were measured by RDI ADCP between 8 and 100 m at 2 m depth intervals, with a 15-min ensemble time interval and 15 pings per ensemble. The ADCP velocity measurement precision and resolution were ± 0.5% and ± 0.1 cm s^{-1}, respectively. The accuracy of the ADCP vertical velocity measurements are not validated, however, the RDI reports that the vertical velocity is more accurate, by at least a factor of two than the horizontal velocity (Wood and Gartner, 2010). The compass accuracy was ± 2° and compass readings were corrected by adding magnetic declination.

The sediment trap was programmed to start a collection at 4 October 2016 0:00 CST with intervals of 35 days for each vial collected. Prior to boarding the vessel, sediment trap preservative density solution was prepared at the Churchill Northern Studies Centre (CNSC). To prepare the solution, 10 L of seawater was collected from the Churchill port wharf and filtered through 0.7 µm Whatman GF/F filters. The salinity of the filtered seawater was adjusted from 26.7 to 37 psu with 88.065 g of ultra-clean sea salt. Borax (44.4 g) was slowly added to 0.45 L of 37% formaldehyde, placed on a magnetic stir plate overnight to dissolve, and decanted into 8.55 L of filtered seawater. Approximately 1 hour before deployment of the sediment traps, pre-acid cleaned vials were placed inside the pre-programmed sampling carrousel and filled to the surface with the preservative solution. The trap was assembled and kept upright prior to and during deployment. During deployment, the different species of zooplankton were captured by the sediment trap (Fig. 6).

3.2 Data Collection and Post Processing

ADCPs, unlike echo-sounders (Lemon et al., 2012, 2001), are limited in deriving accurate quantitative estimates of biomass due to calibration difficulties because their acoustic beams are narrow and inclined from the vertical (Brierley et al., 1998; Lemon et al., 2008; Sato et al., 2013; Vestheim et al., 2014). But with the application of beam geometry correction, ADCPs are commonly used for qualitative studies, as they can provide information on zooplankton presence and behaviour (Hobbs et al., 2014; Last et al., 2016; Petrusevich et al., 2016). To correct for the ADCP beam geometry, we derived the volume backscatter strength (VBS) S_v in dB from echo intensity following the procedure described by *Deines*, (1999).

The total sky illumination for day and night was modelled using *skylight.m* function from the astronomy package for Matlab (Ofek, 2014) and a simple exponential decay radiative transfer model for estimating under ice illumination (Grenfell and Maykut, 1977; Perovich, 1996). Transmittance through the sea ice was calculated following Eq.(1):

$$T(z) = (1 - \alpha)e^{-k_t z}, \quad (1)$$

where α is the surface albedo, κ_t is the bulk extinction coefficient of the sea ice cover, and z is the ice thickness. The values of the coefficients used in the exponential decay model were adjusted for the first-year sea ice: α = 0.8 and κ_t=1.2. We did not have any data for snow cover available, so a presence of the snow cover was omitted in the transmittance model. However, an albedo of 0.8 was used to simulate the high albedo at visible wavelengths for snow-covered or white ice surfaces.

The thickness of ice at the mooring location was estimated from the ice draft evaluated from the distance to the ice-ocean interface measured by the Nortek ADCP (Figure 2) The draft was further transformed to the ice thickness by multiplying 1.115 (Bourke and Paquette, 1989). The acoustic-derived thicknesses were corrected for ADCP tilt, sea surface height and

https://doi.org/10.5194/os-2019-107
Preprint. Discussion started: 7 October 2019

atmospheric pressure (Krishfield et al., 2014) and for the speed of sound. The extreme outliers were excluded, and the mean daily ice thicknesses were calculated for further analysis (Figure 2).

The Environment and Climate Change Canada weather station at Churchill Airport (YYQ) located ~190 km south-west from the mooring location provided wind data for most of the time of mooring deployment, except for the period of March 27 – April 7, 2017. The daily mean wind speed magnitude was used to compile the wind speed time series (Figure 3c).

On recovery of the mooring, sediment trap samples were photographed poured into acid cleaned 250 mL amber glass bottles and stored in the dark at approximately 4 °C during transport to the Centre for Earth Observation Science, University of Manitoba. Samples were poured through 500 µm NITEX mesh sieve to separate the larger zooplankton fraction. Because of this, smaller species, nauplii, eggs and fecal pellets were largely missed from the >500 µm fraction. However, the >500 µm organisms represent the group of zooplankton primarily detected as ADCP backscatter. Zooplankton taxonomy identification was conducted at the Freshwater Institute (DFO) to the lowest taxonomic level possible, enumerated and measured. The entire sample was scanned for large and rare organisms and then the sample was split, with a Motodo box splitter, and a minimum of 300 organisms was counted for each sample.

4. Results

4.1. Ice Thickness, Under-ice Illumination and Wind Data.

At the mooring location, the ice started rapidly forming in the second week of December. By mid-December thickness reached 0.4 m and was gradually growing till the middle of March up to 1 m (Figure 2). Afterwards, the ice thickness at the mooring location varied due to the seasonal factors, e.g. polynyas, sea ice melting, etc.

Modelled under-ice illumination time series, as well as the volume backscatter strength and vertical velocity time series, were presented in the form of actograms (Figures 3d-g and 4). An actogram, being a common method of data display in chronobiological research, has recently been used for displaying zooplankton DVM (Hobbs et al., 2018; Last et al., 2016; Petrusevich et al., 2016; Tran et al., 2016).

The actogram of the modelled under-ice illumination (Figure 3i and 4e) shows continuous daily maximums at noon with minimum values of 2000 lux around the winter solstice and reaching maximum values of 10000 lux in the middle of summer. Maximum under ice lunar illumination was around 0.1 lux during full moon under sea-ice about 0.5 m thick.

4.2 Volume Backscatter Strength (VBS)

For analyzing the depth-dependent behaviour of scatters involved in diurnal vertical migration, we computed the volume backscatter strength (VBS) time series at noon (Figure 3a) and at midnight (Figure 3b). Noon-time series show persistent maximum backscatter strength near the bottom below 92 m depth, which is consistent with DVM. Some scatter stayed at noon at 60-80 m layer during October-January and at 70-80 m in June-July.

https://doi.org/10.5194/os-2019-107
Preprint. Discussion started: 7 October 2019

The near-bottom maximum for the midnight time series of VBS is significantly less compared to that for noon. Midnight time series during October-February and May-July showed a wider spread of scatters over the depth. During winter months (December - February), the thickness of this midnight bottom scatters layer gradually decreased with the growth of sea ice. There are periods of higher VBS at the bottom layer with the same periodicity of 14 days as M_2 and S_2 tidal components superposition maximums (spring tide) throughout the whole time series. There was a seasonal variation of these periodic VBS maxima: they were increasing during summer-fall and decreasing in winter. It should be noted that during November-January there were observed higher values of backscatter below 80 m depth.

VBS was calculated for depths of 8, 20, 60, 80 and 92 m and are shown as actograms in (Figure 3d-h). Overall, VBS actograms shape shows a similar overall shape to that of the under-ice solar illumination actogram (Figure 3i). Reduced under ice illumination from December to March corresponded with reduced VBS through the whole water column, followed by increased illumination during ice breakup and open water periods (April to October) and an increase in VBS within all five depth bins. Like the noon and midnight VBS time series, there is a relatively higher signal at 60, 80 m and 92m depth in November-January during the night.

The VBS actograms (Figure 3d-h) show the presence of vertical bands of higher VBS with 14 days periodicity at multiple depths. In the upper 8 and 20 m (Figure 3d-e), these bands are spreading through the night period, while at 80 and 92 m actograms the bands spread through the whole day with different values of VBS during the day and night. In the 8 m actogram (Figure 3d) there are also non-periodic bands of high backscatter that span from 1 to 5 days in duration. These bands spread throughout the whole day and correspond with the periods of wind speed increasing to strong wind, gale and storm values (30 km/h and up) during the ice-free season (Figure 3c).

Figure 3c shows daily mean wind speed measured at Churchill airport (YYQ). There were observed several periods of mean wind speed higher than 30 km/h, which corresponds with strong wind (37-61 km/h) and gale (62-87 km/h) wind speed values, with maximum wind gusting up to 77 km/h. Normally these storm events lasted from 1 to 6 days.

4.3 Vertical velocity actograms

The vertical velocity actograms were calculated for the same depths as VBS actograms (Figure 4a-d). The seasonal shape of vertical velocity actograms is similar to the shape of under-ice illumination (Figure 3c and 4e) and VBS actograms (Figure 3d-g). The change in vertical speed associated with spring tide is present on the vertical velocity actograms in a form of slanted strips of 14-day periodicity, with amplitude increasing with depth and reaching maximum values in the range of 10-15 mm/s.

The vertical velocity actograms were post-processed to remove the semi-diurnal tidal components (M_2 and S_2) from the vertical velocity data which otherwise would create tidal noise on the actograms (Figure 4f-i). A tidal harmonic analysis was performed for the vertical velocity time series using T_Tide toolbox for Matlab (Pawlowicz et al., 2002). There was a small distinguishable diurnal variation of vertical velocity in 20 and 60 m actograms (Figure 4f and g) during the period of the full moon in October, November and December resembling the slanted shape of lunar illumination at the under-ice illumination actogram (Figure 4e).

https://doi.org/10.5194/os-2019-107
Preprint. Discussion started: 7 October 2019

4.4 Wavelet analysis

Time series of the wavelet power spectrum for the semidiurnal tidal currents were computed for accounting their spring-neap and seasonal variability. Wavelet for horizontal and vertical velocities (Figure 5b and c) show absolute maximum values during spring tides, which is consistent with the full moon and new moon phases (Figure 5a). The power spectrum range for horizontal velocities is, in general, over one order higher than for vertical velocity. There is a difference between horizontal and vertical velocities power spectrum. The horizontal velocities wavelet has maximums that spread through the whole water column during the ice-free season, and below 30 m depth in the presence of ice cover (December-April). The vertical velocities spectrum during October-April has maximums mostly concentrated below 70 m depth. There is seasonal variation for the vertical velocity wavelet with May-June wavelet maximums started spreading through the whole water column.

For the analysis of ADCP measured current velocities, we used wavelet transformation to derive the time-dependent behaviour of horizontal and vertical current velocities at the semi-diurnal tidal frequency band that dominates the backscatter spectrum. In this study, we used the generalized Morse wavelet (with parameters β=100 and γ=3) and jWavelet toolbox (part of jLab toolbox) for signal processing (Lilly, 2017, 2019; Lilly and Gascard, 2006; Lilly and Olhede, 2009).

4.5 Sediment trap zooplankton

Zooplankton (>500) µm captured in the sediment trap samples (Figure 6) were dominated (>98%) by five taxa including two calanoid copepods (*Calanus glacialis* and *Pseudocalanus* spp.), a pelagic sea snail (*Limacina helicina*), a gelatinous arrow worm (*Parasagitta elegans*) and an amphipod (*Themisto libellula*) (Table 1, Figure 7). The abundance of organisms in the trap was generally lowest from March to July with the exception of juvenile (2 mm length) *T. libellua* in bottle 6. The trap samples reflect the presence of >500 µm zooplankton in the water column during the annual cycle. However, species absent from the trap samples (e.g., *L. helicina* in January-March) does not validate absence from the water column.

5. Discussion

5.1 Zooplankton Species Associated with DVM in Hudson Bay

Acoustic backscatter from the single-frequency ADCP do not provide any information on the identity of zooplankton species involved in DVM but signal strength can provide an indication of zooplankton presence provided there is information on the zooplankton species. The zooplankton caught in our sediment trap provide additional information on the zooplankton community composition and its change over the course of the year. Sound is effectively scattered by objects of the size of the wavelength. For 300 kHz ADCP, it is about 5 mm. It is known that zooplankton species with body size less than the wavelength by an order of magnitude (in our case 0.5-5mm) are capable of creating strong backscatter when there is sufficient abundance of them in the water column (Cisewski and Strass, 2016; Pinot and Jansá, 2001). The backscatter strength of zooplankton species also depends on their acoustic properties, such as shape, internal structure, orientation in the water column and body

https://doi.org/10.5194/os-2019-107
Preprint. Discussion started: 7 October 2019

composition, that causes a difference between the speed of sound in their bodies and surrounding seawater (Stanton et al., 1994, 1998a, 1998b). For example, the species with hard shells (like *Limacina helicina*) and gaseous enclosures scatter sound stronger than gelatinous ones (Lavery et al., 2007; Warren and Wiebe, 2008).

The most abundant species from the zooplankton trap catch (*Parasagita elegans*, *Pseudocalanus* and *L. helicina*) had lengths of 20-30 mm, 0.6-1.4 mm and 0.4-2 mm respectively. Less abundant species from the trap (*Calanus glacialis* and *Themisto libellula*) had lengths of 2.8-4.2 mm and 7.2-31.8 mm, respectively. *P. elegans* and *T. libellula* lengths are in the range of ADCP wavelength and thus should effectively act as scatters. Lengths of *C. glacialis*, *Pseudocalanus* and *L. helicina* are less than the wavelength by an order of magnitude. However, their abundance in the water column during open water season (Estrada et al., 2012) is high enough (>1000 ind m^3) to expect a backscatter signal. *L. helicina's* hard shell should be another contributing factor to backscatter strength. Therefore, we assume that all the species identified in the sediment trap could act as acoustic scatters contributing to the VBS signal analyzed in this study.

The ADCP analyses indicate that zooplankton in Hudson Bay undergo both seasonal and diel migration. This is similar to measured seasonal migration by copepod species in the southern Arctic Ocean and in Rijpfjorden in Svalbard (Falk-Petersen et al., 2008). Seasonal migration is occurring in Hudson Bay despite shallower overwintering waters than in Svalbard and the Beaufort Sea. The observed diel migration in Hudson Bay is similar to other Arctic locations (Berge et al., 2014, 2015a; Hobbs et al., 2018; Last et al., 2016; Petrusevich et al., 2016) suggesting that DVM is an important consideration for carbon/nitrogen transfer within the relatively shallow Hudson Bay system.

Zooplankton species identified from the sediment trap suggest that multiple species could be involved in the DVM. The identification of individual species involved in DVM is not currently possible and is challenged by issues such as the overlapping of signals. Comparison between acoustic and net data in Kongsfjorden, Svalbard led to the conclusion that the acoustic backscatter signal from numerically dominant *Calanus* copepods is typically overwhelmed by the signal from larger and less abundant zooplankton species, such as *Themisto* (Berge et al., 2014). Large copepods (like *Calanus* spp.) and chaetognaths (*P. elegans*) were observed performing diel migrations in Kongsfjorden (Darnis et al., 2017). While our sediment trap showed the prevalence of gelatinous zooplankton species (Fig. 7 – *P. elegans*), but the detection of their migration by ADCP backscattering could be underestimated because gelatinous species are weak scatters.

Regardless, there is an important pump of carbon/nitrogen occurring within Hudson Bay based on zooplankton DMV, and seasonal differences (discussed in next section) could impact this vertical energy transfer. Here, we are not in a position to quantify the biomass involved in the DVM but focus on understanding its pattern. In the next section 5.2, we discuss changes in DVM seasonal cycle, sea-ice cover and modelled under-ice illuminance. We then describe the disruption of DVM in the upper layer by wind storms (section 5.3), and finally DVM interaction with the tide (section 5.4).

5.2 DVM seasonal cycle, sea-ice cover and under-ice illuminance

The mooring site is located 6° south of the Arctic circle and polar twilight zone, which is more southern location compared to other sea-ice covered Arctic and sub-Arctic regions where DVM during winter ice-covered period was observed and was

https://doi.org/10.5194/os-2019-107
Preprint. Discussion started: 7 October 2019

controlled by the lunar light (Last et al., 2016; Petrusevich et al., 2016). In this study, DVM was generally controlled by solar illumination throughout the whole year, which is evident from the shape of VBS (Figure 3d-h) and vertical velocity actograms (Figure 4). The actograms are nearly symmetric around astronomic midnight (dashed horizontal line, Figures 3 and 4), and winter and summer solstice.

The noon-time VBS time series showed consistent maximum backscatter strength below 92 m depth (Figure 3a). Compared to the midnight time series (Figure 3b), it is clear that the backscatter was associated with DVM rather than sediment resuspension caused by the lunar semi-diurnal M_2 tide with a period of 12 hours 25 minutes. The midnight VBS time series (Figure 3b) and VBS actograms (Figures 3d-h) confirm that the zooplankton were aggregated in the upper water column at midnight, likely feeding.

Seasonal variations in zooplankton migration and distribution in the water column were observed throughout the entire time series. The sediment trap at 85 m depth may have captured zooplankton species migrating vertically and possibly also individuals sinking to the bottom (Figure 6). The strong VBS of –70dB during noon at the 90-100 m depth layer (Figure 3a), compared with –80dB at midnight (Figure 3b), suggests that noon-time DVM-associated zooplankton biomass was primarily located at the bottom layer through the annual cycle. From October to the middle of January, however, there was a layer of VBS in the range of –80 to –75dB at 60-80m depth, which can be interpreted that some of the zooplankton were staying at that depth instead of migrating all the way down to the bottom for daytime or to the surface at night. The 60-80 m aggregation of zooplankton, from October to January, corresponds with the first three sampling bottles of the sediment trap when there was the highest abundance of zooplankton species observed with the abundance of dominant species per 35-day sampling period, decreasing from 720 down to 250 ind m^{-3} (Figure 7). From the middle of January to early May, most of the zooplankton biomass at midnight did not migrate above 60 m depth. From May to July zooplankton returned to the vertical migration pattern observed from date to date when zooplankton remained near the bottom at noon and migrates to the surface at night. In July, some zooplankton stayed in the surface layer at noon. This corresponds to the beginning of the ice-free season (Figure 2) when long daylight and abundance of phytoplankton disrupts DVM. Once the sea ice was completely gone in early August, there was a change in zooplankton distribution in the water column. During midnight, some zooplankton remained at the bottom and while others migrated to the surface layer likely feeding during the short night and moving back down to the bottom for the light time. This suggests that different zooplankton scatter species and/or size classes are responding differently to both solar cues and ice cover.

5.3 Disruption of DVM signal in the upper layer by storms

The 8 m depth actogram (Figure 3d) shows several bands of higher VBS of different durations, that are not observed at the deeper layers. These bands spread throughout the entire 24-hour day for a duration of one to several days. These bands (Figure 3d) nicely correspond with daily mean wind speed exceeding 25 km/h (Figure 3c) during most of the ice-free season (October-mid December 2016 and September-October 2017). Irregular spots of higher VBS can be related to the bubbling generated by the wind forcing. In contrast, during the ice-covered season, periods of high winds did not associate with higher VBS. For

https://doi.org/10.5194/os-2019-107
Preprint. Discussion started: 7 October 2019

example, on 7-10 March 2017, the daily mean wind was to 66 km/h, but there were no bands of higher VBS at the 8 m actogram (Figure 3d), indicating that present ice cover partly protected the water column from wind stress. Irregular spots of higher VBS (Figure 3d) during the ice-covered period (February-March) could be attributed to the frazil ice formation. With the onset of spring melt (May-July), there is also more noise-type VBS that could be attributed to the release of the ice-rafted sediments during the melting of the sea ice. The large amount in sediment present in the May-July sediment trap bottles (Figure 6) provide proof for the presence of sinking sediment during this period.

5.4 Disruption of DVM by the spring tide

Time series of the wavelet power spectrum for horizontal and vertical velocities (Figures 5b, c) show absolute maximum values during spring tides, which correspond to full moon and new moon phases (Figure 5a). For 92 m depth, the 14-day running correlation (Figure 5d, green line) between VBS (blue line) and vertical velocity wavelet (red line) was calculated. Correlations exceeding ±0.53 are statistically significant at the 95% confidence level (Figure 5d, yellow shading). Pink shading identifies the events when this statistically significant correlation was observed. The periods of low correlation were from the end of November to mid-January, mid-February to mid-March, April to mid-June and the first half of September. A statistically significant positive correlation suggests the relationship between VBS and tidal forcing.

In the presence of background stratification, the barotropic tide interacts with sloping bottom topography in the proximity of the mooring location (Figure 1), which is typical for Hudson Bay (Petrusevich et al., 2018). This interaction generates vertical divergence and convergence of tidal flow, resulting in the depth-dependent behaviour of the vertical velocity at a tidal frequency here defined as the baroclinic tide. Seasonal character of the baroclinic tide can also be affected by density stratification. During May-October 2017 the vertical velocity wavelet maximums were amplified (Figure 5c). During this period there were DVM disruptions throughout the water column that are clearly evident on VBS actograms (Figures 3d-g) and at noon VBS time series (Figure 3a).

Zooplankton normally avoid spending additional energy to cross such an interface a horizontal interface with a strong velocity gradient, thereby resulting in a weakened or absence of a DVM signal (Petrusevich et al., 2016). Similar observations of disrupted zooplankton vertical migration had been linked to upwelling and downwelling events (Dmitrenko et al., 2019). The same considerations can be applied to this study when water dynamics are impacted by vertical currents generated by the baroclinic tides and enhanced during spring tide. During spring tide, zooplankton showed a weakened DVM to avoid moving against the vertically diverging and converging tidal flow, as follows from the VBS actograms and correlation between time series of VBS and vertical velocity wavelet. This disruption can be moon controlled as those reported by Hobbs et al. (2014); Last et al. (2016), and Petrusevich et al. (2016). However, in this study, the lunar origin of this disruption is attributed to the tidal dynamics rather than the moonlight, because disruptions occurred during the full moon and new moon phases.

https://doi.org/10.5194/os-2019-107
Preprint. Discussion started: 7 October 2019

6. Conclusion

A one-year-long acoustic backscatter and vertical velocity time series, obtained using a 300 kHz ADCP on a mooring deployed from September 2016 to October 2017 in south-east Hudson Bay (~190 km north-east from the port of Churchill), revealed a distinct diurnal pattern consistent with zooplankton diel vertical migration (DVM).

In this study, we were able to identify that the presence of multiple zooplankton species that could have been involved in DVM from samples collected by the sediment trap. The sediment trap was programmed to collect settling material over a complete annual cycle (35-day interval and averaging period) and consequently, the collection was not timed to shorter tidal cycles. This limited the identification of the specific species whose DVM was detected by the 300 kHz ADCP and altered by M_2 tidal water dynamics. Using shorter sediment trap time intervals or in situ sampling required for the identification of the zooplankton species involved in DVM in future mooring deployments.

The major factors determining the observed DVM pattern were as follows:

Illuminance. Unlike other ice-covered and ice-free Arctic and sub-Arctic locations such as Svalbard and north-east Greenland (Last et al., 2016; Petrusevich et al., 2016), DVM in Hudson Bay is controlled by solar illumination throughout the whole year, not by moonlight.

Tidal dynamics. The tide in Hudson Bay is mostly lunar semidiurnal (M_2) with an amplitude of about a few meters. The area in the proximity of the mooring has variable bottom topography (Figure 1). The barotropic tide interacts with bottom topography generating tidal flow diverging and converging vertically. It seems that zooplankton tends to avoid spending additional energy swimming against the vertical flow. This response of zooplankton is consistent with the zooplankton tendency to stay away from the layers with enhanced water dynamics and to adjust its DVM accordingly.

Storm induced disruptions. When daily mean wind speed exceeded 25 km/h during most of the ice-free season in the surface layer there were observed irregular spots of higher VBS related to the bubbling generated by the wind forcing.

Data and code availability

The backscatter and velocity data are archived in the Centre for Earth Observation Science (University of Manitoba) and are restricted for open access in accordance with University of Manitoba policy during two years after the observations completed. The Matlab code used for data processing is available from VP upon request.

Authors contribution

VP prepared the manuscript with contributions from all co-authors (ID, AN, SK, MK, ZK, DB and JE). VP, SK and MK deployed and retrieved the mooring in Hudson Bay. AN processed and presented zooplankton data from the sediment trap. VP processed and presented acoustic data from the ADCP. SK processed and provided data for the ice draft.

https://doi.org/10.5194/os-2019-107
Preprint. Discussion started: 7 October 2019

Competing interests

The authors declare that they have no conflict of interest.

Acknowledgements

Funding support from BaySys (Hudson Bay System Study), the Natural Sciences and Engineering Research Council (NSERC), Discovery Grant program, and the ArcticNet Network of Centres of Excellence made field data collection and analysis possible. We also acknowledge contributions from the Canada Excellence Research Chair (CERC) and Canada Research Chair (CRC) programs to support the University of Manitoba team. We would like to give special thanks to Alexis Burt of Fisheries and Oceans Canada for processing zooplankton taxa. We would like to thank the Captain, Chief Officer Kevin Jones and crew of the CCGS Henry Larsen, the Canadian Coast Guard, technician Sylvan Blondeau of Laval University and Christopher Peck of the University of Manitoba for their assistance with successful mooring retrieval, as well Nathalie Thériault for coordinating BaySys field logistics.

References

Baker, E. T. and Milburn, H. B.: An instrument system for the investigation of particle fluxes, Cont. Shelf Res., 1(4), 425–435, doi:10.1016/0278-4343(83)90006-7, 1983.

Bandara, K., Varpe, Ø., JE, S., Wallenschus, J., Berge, J. and Eiane, K.: Seasonal vertical strategies in a high-Arctic coastal zooplankton community, Mar. Ecol. Prog. Ser., 555, 49–64 [online] Available from: http://www.int-res.com/abstracts/meps/v555/p49-64/, 2016.

Båtnes, A. S., Miljeteig, C., Berge, J., Greenacre, M. and Johnsen, G.: Quantifying the light sensitivity of Calanus spp. during the polar night: potential for orchestrated migrations conducted by ambient light from the sun, moon, or aurora borealis?, Polar Biol., 38(1), 51–65, doi:10.1007/s00300-013-1415-4, 2015.

Benoit, D., Simard, Y., Gagné, J., Geoffroy, M. and Fortier, L.: From polar night to midnight sun: photoperiod, seal predation, and the diel vertical migrations of polar cod (Boreogadus saida) under landfast ice in the Arctic Ocean, Polar Biol., 33(11), 1505–1520, doi:10.1007/s00300-010-0840-x, 2010.

Berge, J., Cottier, F., Last, K. S., Varpe, Ø., Leu, E., Søreide, J., Eiane, K., Falk-Petersen, S., Willis, K., Nygård, H., Vogedes, D., Griffiths, C., Johnsen, G., Lorentzen, D. and Brierley, A. S.: Diel vertical migration of Arctic zooplankton during the polar night., Biol. Lett., 5(1), 69–72, doi:10.1098/rsbl.2008.0484, 2009.

Berge, J., Båtnes, A. S., Johnsen, G., Blackwell, S. M. and Moline, M. A.: Bioluminescence in the high Arctic during the polar night., Mar. Biol., 159(1), 231–237, doi:10.1007/s00227-011-1798-0, 2012.

Berge, J., Cottier, F., Varpe, O., Renaud, P. E., Falk-Petersen, S., Kwasniewski, S., Griffiths, C., Søreide, J. E., Johnsen, G.,

https://doi.org/10.5194/os-2019-107
Preprint. Discussion started: 7 October 2019

Aubert, A., Bjærke, O., Hovinen, J., Jung-Madsen, S., Tveit, M. and Majaneva, S.: Arctic complexity: a case study on diel vertical migration of zooplankton., J. Plankton Res., 36(5), 1279–1297, doi:10.1093/plankt/fbu059, 2014.

Berge, J., Renaud, P. E., Darnis, G., Cottier, F., Last, K., Gabrielsen, T. M., Johnsen, G., Seuthe, L., Weslawski, J. M., Leu, E., Moline, M., Nahrgang, J., Søreide, J. E., Varpe, Ø., Lønne, O. J., Daase, M. and Falk-Petersen, S.: In the dark: a review of ecosystem processes during the Arctic polar night, Prog. Oceanogr., 139, 258–271, doi:10.1016/j.pocean.2015.08.005, 2015a.

Berge, J., Daase, M., Renaud, P. E., Ambrose, W. G., Darnis, G., Last, K. S., Leu, E., Cohen, J. H., Johnsen, G., Moline, M. A., Cottier, F., Varpe, Ø., Shunatova, N., Bałazy, P., Morata, N., Massabuau, J.-C., Falk-Petersen, S., Kosobokova, K., Hoppe, C. J. M., Węsławski, J. M., Kukliński, P., Legeżyńska, J., Nikishina, D., Cusa, M., Kędra, M., Włodarska-Kowalczuk, M., Vogedes, D., Camus, L., Tran, D., Michaud, E., Gabrielsen, T. M., Granovitch, A., Gonchar, A., Krapp, R. and Callesen, T. A.: Unexpected Levels of Biological Activity during the Polar Night Offer New Perspectives on a Warming Arctic, Curr. Biol., 25(19), 2555–2561, doi:10.1016/j.cub.2015.08.024, 2015b.

Blachowiak-Samolyk, K., Kwasniewski, S., Richardson, K., Dmoch, K., Hansen, E., Hop, H., Falk-Petersen, S. and Mouritsen, L. T.: Arctic zooplankton do not perform diel vertical migration (DVM) during periods of midnight sun, Mar. Ecol. Prog. Ser., 308(Dvm), 101–116, doi:10.3354/meps308101, 2006.

Bourke, R. H. and Paquette, R. G.: Estimating the thickness of sea ice, J. Geophys. Res. Ocean., 94(C1), 919–923, doi:10.1029/JC094iC01p00919, 1989.

Bozzano, R., Fanelli, E., Pensieri, S., Picco, P. and Schiano, M. E.: Temporal variations of zooplankton biomass in the Ligurian Sea inferred from long time series of ADCP data, Ocean Sci., 10(1), 93–105, doi:10.5194/os-10-93-2014, 2014.

Brierley, A. S.: Diel vertical migration, Curr. Biol., 24(22), R1074–R1076, doi:10.1016/j.cub.2014.08.054, 2014.

Brierley, A. S., Brandon, M. A. and Watkins, J. L.: An assessment of the utility of an acoustic Doppler current profiler for biomass estimation, Deep Sea Res. Part I Oceanogr. Res. Pap., 45(9), 1555–1573, doi:10.1016/S0967-0637(98)00012-0, 1998.

Brierley, A. S., Saunders, R. A., Bone, D. G., Murphy, E. J., Enderlein, P., Conti, S. G. and Demer, D. A.: Use of moored acoustic instruments to measure short-term variability in abundance of Antarctic krill, Limnol. Oceanogr. Methods, 4(2), 18–29, doi:10.4319/lom.2006.4.18, 2006.

Burt, W. J., Thomas, H., Miller, L. A., Granskog, M. A., Papakyriakou, T. N. and Pengelly, L.: Inorganic carbon cycling and biogeochemical processes in an Arctic inland sea (Hudson Bay), Biogeosciences, 13(16), 4659–4671, doi:10.5194/bg-13-4659-2016, 2016.

Carmack, E. and Wassmann, P.: Food webs and physical-biological coupling on pan-Arctic shelves: Unifying concepts and comprehensive perspectives, Prog. Oceanogr., 71(2–4), 446–477, doi:10.1016/j.pocean.2006.10.004, 2006.

Cisewski, B. and Strass, V. H.: Acoustic insights into the zooplankton dynamics of the eastern Weddell Sea, Prog. Oceanogr., 144, 62–92, doi:10.1016/j.pocean.2016.03.005, 2016.

Cisewski, B., Strass, V. H., Rhein, M. and Krägefsky, S.: Seasonal variation of diel vertical migration of zooplankton from ADCP backscatter time series data in the Lazarev Sea, Antarctica, Deep. Res. Part I Oceanogr. Res. Pap., 57(1), 78–94, doi:10.1016/j.dsr.2009.10.005, 2010.

https://doi.org/10.5194/os-2019-107
Preprint. Discussion started: 7 October 2019

Cohen, J. H., Berge, J., Moline, M. a., Sørensen, A. J., Last, K., Falk-Petersen, S., Renaud, P. E., Leu, E. S., Grenvald, J., Cottier, F., Cronin, H., Menze, S., Norgren, P., Varpe, Ø., Daase, M., Darnis, G. and Johnsen, G.: Is Ambient Light during the High Arctic Polar Night Sufficient to Act as a Visual Cue for Zooplankton?, PLoS One, 10(6), e0126247, doi:10.1371/journal.pone.0126247, 2015.

Conover, R. J. and Huntley, M.: Copepods in ice-covered seas—Distribution, adaptations to seasonally limited food, metabolism, growth patterns and life cycle strategies in polar seas, J. Mar. Syst., 2(1), 1–41, doi:https://doi.org/10.1016/0924-7963(91)90011-I, 1991.

Cottier, F. R., Tarling, G. a., Wold, A. and Falk-Petersen, S.: Unsynchronized and synchronized vertical migration of zooplankton in a high arctic fjord, Limnol. Oceanogr., 51(6), 2586–2599, doi:10.4319/lo.2006.51.6.2586, 2006.

Darnis, G., Hobbs, L., Geoffroy, M., Grenvald, J. C., Renaud, P. E., Berge, J., Cottier, F., Kristiansen, S., Daase, M., E. Søreide, J., Wold, A., Morata, N. and Gabrielsen, T.: From polar night to midnight sun: Diel vertical migration, metabolism and biogeochemical role of zooplankton in a high Arctic fjord (Kongsfjorden, Svalbard), Limnol. Oceanogr., 62(4), 1586–1605, doi:10.1002/lno.10519, 2017.

Deines, K. L.: Backscatter estimation using Broadband acoustic Doppler current profilers, in Proceedings of the IEEE Sixth Working Conference on Current Measurement, pp. 249–253, IEEE, San Diego, CA., 1999.

Dmitrenko, I. A., Petrusevich, V., Darnis, G., Kirillov, S. A., Komarov, A. S., Ehn, J. K., Forest, A., Fortier, L., Rysgaard, S. and Barber, D. G.: Sea-ice and water dynamics and moonlight impact the acoustic backscatter diurnal signal over the eastern Beaufort Sea continental slope, Manuscr. Submitt. Publ., 2019.

Doney, S. C. and Steinberg, D. K.: Marine biogeochemistry: The ups and downs of ocean oxygen, Nat. Geosci., 6(7), 515–516, doi:10.1038/ngeo1872, 2013.

Estrada, R., Harvey, M., Gosselin, M., Starr, M., Galbraith, P. S. and Straneo, F.: Late-summer zooplankton community structure, abundance, and distribution in the Hudson Bay system (Canada) and their relationships with environmental conditions, 2003–2006, Prog. Oceanogr., 101(1), 121–145, doi:https://doi.org/10.1016/j.pocean.2012.02.003, 2012.

Falk-Petersen, S., Leu, E., Berge, J., Kwasniewski, S., Nygård, H., Røstad, A., Keskinen, E., Thormar, J., von Quillfeldt, C., Wold, A. and Gulliksen, B.: Vertical migration in high Arctic waters during autumn 2004, Deep Sea Res. Part II Top. Stud. Oceanogr., 55(20–21), 2275–2284, doi:10.1016/j.dsr2.2008.05.010, 2008.

Ferland, J., Gosselin, M. and Starr, M.: Environmental control of summer primary production in the Hudson Bay system: The role of stratification, J. Mar. Syst., 88(3), 385–400, doi:https://doi.org/10.1016/j.jmarsys.2011.03.015, 2011.

Fielding, S., Griffiths, G. and Roe, H. S. J.: The biological validation of ADCP acoustic backscatter through direct comparison with net samples and model predictions based on acoustic-scattering models, ICES J. Mar. Sci. J. du Cons., 61(2), 184–200, doi:10.1016/j.icesjms.2003.10.011, 2004.

Fortier, M.: Visual predators and the diel vertical migration of copepods under Arctic sea ice during the midnight sun, J. Plankton Res., 23(11), 1263–1278, doi:10.1093/plankt/23.11.1263, 2001.

Gagnon, A. S. and Gough, W. A.: Trends in the dates of ice freeze-up and breakup over Hudson Bay, Canada, Arctic, 58(4),

370–382, doi:10.14430/arctic451, 2005.

Gagnon, A. S. and Gough, W. A.: East-west asymmetry in long-term trends of landfast ice thickness in the Hudson Bay region, Canada, Clim. Res., 32(3), 177–186, doi:10.3354/cr032177, 2006.

Grenfell, C. G. and Maykut, G. a: The optical properties of ice and snow in the Arctic Basin, J. Glaciol., 18(80), 445–463 [online] Available from: http://www.igsoc.org/journal.old/18/80/igs_journal_vol18_issue080_pg445-463.pdf, 1977.

Guerra, D., Schroeder, K., Borghini, M., Camatti, E., Pansera, M., Schroeder, A., Sparnocchia, S. and Chiggiato, J.: Zooplankton diel vertical migration in the Corsica Channel (north-western Mediterranean Sea) detected by a moored acoustic Doppler current profiler, Ocean Sci., 15(3), 631–649, doi:10.5194/os-15-631-2019, 2019.

Hays, G. C.: A review of the adaptive significance and ecosystem consequences of zooplankton diel vertical migrations, Hydrobiologia, 503(1–3), 163–170, doi:10.1023/B:HYDR.0000008476.23617.b0, 2003.

Hill, A. E.: Vertical migration in tidal currents, Mar. Ecol. Prog. Ser., 75(1), 39–54, doi:10.3354/meps075039, 1991.

Hill, A. E.: Horizontal zooplankton dispersal by diel vertical migration in S2 tidal currents on the northwest European continental shelf, Cont. Shelf Res., 14(5), 491–506, doi:10.1016/0278-4343(94)90100-7, 1994.

Hobbs, L., Cottier, F. R., Last, K. S. and Berge, J.: Pan-Arctic diel vertical migration during the polar night, Mar. Ecol. Prog. Ser., 605, 61–72 [online] Available from: https://www.int-res.com/abstracts/meps/v605/p61-72/, 2018.

Hobbs, L. J., Cottier, F. R., Last, K. S. and Berge, J.: Environmental controls on winter Diel Vertical Migration behaviour in the high Arctic using eight years of acoustic data, in Arcic Change, Ottawa., 2014.

Hochheim, K. P. and Barber, D. G.: An Update on the Ice Climatology of the Hudson Bay System, Arctic, Antarct. Alp. Res., 46(1), 66–83, doi:10.1657/1938-4246-46.1.66, 2014.

Jones, E. P., Swift, J. H., Anderson, L. G., Lipizer, M., Civitarese, G., Falkner, K. K., Kattner, G. and McLaughlin, F.: Tracing Pacific water in the North Atlantic Ocean, J. Geophys. Res. Ocean., 108(C4), doi:10.1029/2001JC001141, 2003.

Josenhans, H. W. and Zevenhuizen, J.: Dynamics of the Laurentide Ice Sheet in Hudson Bay, Canada, Mar. Geol., 92(1), 1–26, doi:https://doi.org/10.1016/0025-3227(90)90024-E, 1990.

Kosobokova, K. N.: Diurnal Vertical Distribution Of Calanus Hyperboreus Kroyer And Calanus Glacialis Jaschnov In Central Polar Basin, Okeanologiya, 18(4), 722–728, 1978.

Krishfield, R. A., Proshutinsky, A., Tateyama, K., Williams, W. J., Carmack, E. C., MaLaughlin, F. A. and Timmermans, M.-L.: Deterioration of perennial sea ice in the Beaufort Gyre from 2003 to 2012 and its impact on the oceanic freshwater cycle, J. Geophys. Res. Ocean., 119(2), 1271–1305, doi:10.1002/2013JC008999, 2014.

Lampert, W.: The Adaptive Significance of Diel Vertical Migration of Zooplankton, Funct. Ecol., 3, 21–27, 1989.

Landy, J. C., Ehn, J. K., Babb, D. G., Thériault, N. and Barber, D. G.: Sea ice thickness in the Eastern Canadian Arctic: Hudson Bay Complex & Baffin Bay, Remote Sens. Environ., 200(Supplement C), 281–294, doi:https://doi.org/10.1016/j.rse.2017.08.019, 2017.

Last, K. S., Hobbs, L., Berge, J., Brierley, A. S. and Cottier, F.: Moonlight Drives Ocean-Scale Mass Vertical Migration of Zooplankton during the Arctic Winter, Curr. Biol., 26(2), 244–251, doi:10.1016/j.cub.2015.11.038, 2016.

https://doi.org/10.5194/os-2019-107
Preprint. Discussion started: 7 October 2019

Lavery, A. C., Wiebe, P. H., Stanton, T. K., Lawson, G. L., Benfield, M. C. and Copley, N.: Determining dominant scatterers of sound in mixed zooplankton populations, J. Acoust. Soc. Am., 122(6), 3304–3326, doi:10.1121/1.2793613, 2007.

Lemon, D., Johnston, P., Buermans, J., Loos, E., Borstad, G. and Brown, L.: Multiple-frequency moored sonar for continuous observations of zooplankton and fish, in 2012 Oceans, pp. 1–6., 2012.

Lemon, D. D., Gower, J. F. R. and Clarke, M. R.: The acoustic water column profiler: a tool for long-term monitoring of zooplankton populations, in MTS/IEEE Oceans 2001. An Ocean Odyssey. Conference Proceedings (IEEE Cat. No.01CH37295), vol. 3, pp. 1904–1909 vol.3., 2001.

Lemon, D. D., Billenness, D. and Buermans, J.: Comparison of acoustic measurements of zooplankton populations using an Acoustic Water Column Profiler and an ADCP, in OCEANS 2008, pp. 1–8, IEEE Oceanic Engineering Society, Quebec City, QC., 2008.

Lilly, J. M.: Element analysis: a wavelet-based method for analysing time-localized events in noisy time series, Proc. R. Soc. A Math. Phys. Eng. Sci., 473(2200), 20160776, doi:10.1098/rspa.2016.0776, 2017.

Lilly, J. M.: jLab: A data analysis package for Matlab, [online] Available from: http://www.jmlilly.net/jmlsoft.html, 2019.

Lilly, J. M. and Gascard, J.-C.: Wavelet ridge diagnosis of time-varying elliptical signals with application to an oceanic eddy, Nonlinear Process. Geophys., 13(5), 467–483, doi:10.5194/npg-13-467-2006, 2006.

Lilly, J. M. and Olhede, S. C.: Higher-Order Properties of Analytic Wavelets, IEEE Trans. Signal Process., 57(1), 146–160, doi:10.1109/TSP.2008.2007607, 2009.

Ofek, E. O.: MATLAB package for astronomy and astrophysics, Astrophys. Source Code Libr. Rec. ascl1407.005, doi:2014ascl.soft07005O, 2014.

Pawlowicz, R., Beardsley, B. and Lentz, S.: Classical tidal harmonic analysis including error estimates in MATLAB using T_TIDE, Comput. Geosci., 28(8), 929–937, doi:10.1016/S0098-3004(02)00013-4, 2002.

Perovich, D. K.: The Optical Properties of Sea Ice, CRREL Monogr., 96–1(May 1996), 25 [online] Available from: http://www.dtic.mil/cgi-bin/GetTRDoc?AD=ADA310586&Location=U2&doc=GetTRDoc.pdf, 1996.

Petrusevich, V., Dmitrenko, I. A., Kirillov, S. A., Rysgaard, S., Falk-Petersen, S., Barber, D. G., Boone, W. and Ehn, J. K.: Wintertime water dynamics and moonlight disruption of the acoustic backscatter diurnal signal in an ice-covered Northeast Greenland fjord, J. Geophys. Res. Ocean., 121(7), 4804–4818, doi:10.1002/2016JC011703, 2016.

Petrusevich, V. Y., Dmitrenko, I. A., Kozlov, I. E., Kirillov, S. A., Kuzyk, Z. Z. A., Komarov, A. S., Heath, J. P., Barber, D. G. and Ehn, J. K.: Tidally-generated internal waves in Southeast Hudson Bay, Cont. Shelf Res., 167, 65–76, doi:10.1016/j.csr.2018.08.002, 2018.

Pinot, J. M. and Jansá, J.: Time variability of acoustic backscatter from zooplankton in the Ibiza Channel (western Mediterranean), Deep. Res. Part I Oceanogr. Res. Pap., 48, 1651–1670, doi:10.1016/S0967-0637(00)00095-9, 2001.

Potiris, E., Frangoulis, C., Kalampokis, A., Ntoumas, M., Pettas, M., Petihakis, G. and Zervakis, V.: Acoustic Doppler current profiler observations of migration patterns of zooplankton in the Cretan Sea, Ocean Sci., 14(4), 783–800, doi:10.5194/os-14-783-2018, 2018.

Prinsenberg, S. J.: Seasonal current variations observed in western Hudson Bay, J. Geophys. Res. Ocean., 92(C10), 756–766, doi:10.1029/JC092iC10p10756, 1987.

Prinsenberg, S. J. and Freeman, N. G.: Tidal heights and currents in Hudson Bay and James Bay, in Canadian Inland Seas, vol. 44, edited by I. P. Martini, pp. 205–216, Elsevier Science., 1986.

Rabindranath, A., Daase, M., Falk-Petersen, S., Wold, A., Wallace, M. I., Berge, J. and Brierley, A. S.: Seasonal and diel vertical migration of zooplankton in the High Arctic during the autumn midnight sun of 2008, Mar. Biodivers., 41(3), 365–382, doi:10.1007/s12526-010-0067-7, 2010.

Ray, R. D.: On Measurements of the Tide at Churchill, Hudson Bay, Atmosphere-Ocean, 54(2), 108–116, doi:10.1080/07055900.2016.1139540, 2016.

Ringelberg, J.: Migrations in the Marine Environment, in Diel Vertical Migration of Zooplankton in Lakes and Oceans: Causal Explanations and Adaptive Significances, pp. 217–249, Springer Netherlands., 2010.

Sato, M., Dower, J. F., Kunze, E. and Dewey, R.: Second-order seasonal variability in diel vertical migration timing of euphausiids in a coastal inlet, Mar. Ecol. Prog. Ser., 480, 39–56, doi:10.3354/meps10215, 2013.

Saucier, F. J., Senneville, S., Prinsenberg, S., Roy, F., Smith, G., Gachon, P., Caya, D. and Laprise, R.: Modelling the sea ice-ocean seasonal cycle in Hudson Bay, Foxe Basin and Hudson Strait, Canada, Clim. Dyn., 23(3–4), 303–326, doi:10.1007/s00382-004-0445-6, 2004.

St-Laurent, P., Saucier, F. J. and Dumais, J. F.: On the modification of tides in a seasonally ice-covered sea, J. Geophys. Res. Ocean., 113(11), 1–11, doi:10.1029/2007JC004614, 2008.

Stanton, T. K., Wiebe, P. H., Chu, D., Benfield, M. C., Scanlon, L., Martin, L. and Eastwood, R. L.: On acoustic estimates of zooplankton biomass, ICES J. Mar. Sci. J. du Cons., 51(4), 505–512, doi:10.1006/jmsc.1994.1051, 1994.

Stanton, T. K., Chu, D. Z., Wiebe, P. H., Martin, L. V and Eastwood, R. L.: Sound scattering by several zooplankton groups. I. Experimental determination of dominant scattering mechanisms, J. Acoust. Soc. Am., 103(1), 225–235, doi:10.1121/1.421469, 1998a.

Stanton, T. K., Chu, D. Z. and Wiebe, P. H.: Sound scattering by several zooplankton groups. II. Scattering models, J. Acoust. Soc. Am., 103(1), 236–253, doi:10.1121/1.421110, 1998b.

Torgersen, T.: Proximate causes for anti-predatory feeding suppression by zooplankton during the day: reduction of contrast or motion--ingestion or clearance?, J. Plankton Res., 25(5), 565–571, doi:10.1093/plankt/25.5.565, 2003.

Tran, D., Sow, M., Camus, L., Ciret, P., Berge, J. and Massabuau, J.-C.: In the darkness of the polar night, scallops keep on a steady rhythm, Sci. Rep., 6, 32435 [online] Available from: http://dx.doi.org/10.1038/srep32435, 2016.

Valle-Levinson, A., Castro, L., Cáceres, M. and Pizarro, O.: Twilight vertical migrations of zooplankton in a Chilean fjord, Prog. Oceanogr., 129, 114–124, doi:https://doi.org/10.1016/j.pocean.2014.03.008, 2014.

Varpe, Ø.: Fitness and phenology: Annual routines and zooplankton adaptations to seasonal cycles, J. Plankton Res., 34(4), 267–276, doi:10.1093/plankt/fbr108, 2012.

Vestheim, H., Røstad, A., Klevjer, T. A., Solberg, I. and Kaartvedt, S.: Vertical distribution and diel vertical migration of krill

beneath snow-covered ice and in ice-free waters., J. Plankton Res., 36(2), 503–512, doi:10.1093/plankt/fbt112, 2014.

Wallace, M. I., Cottier, F. R., Berge, J., Tarling, G. a., Griffiths, C. and Brierley, A. S.: Comparison of zooplankton vertical migration in an ice-free and a seasonally ice-covered Arctic fjord: An insight into the influence of sea ice cover on zooplankton behaviour, Limnol. Oceanogr., 55(2), 831–845, doi:10.4319/lo.2009.55.2.0831, 2010.

Wang, H., Chen, H., Xue, L., Liu, N. and Liu, Y.: Zooplankton diel vertical migration and influence of upwelling on the biomass in the Chukchi Sea during summer, Acta Oceanol. Sin., 34(5), 68–74, doi:10.1007/s13131-015-0668-x, 2015.

Warren, J. D. and Wiebe, P. H.: Accounting for biological and physical sources of acoustic backscatter improves estimates of zooplankton biomass, Can. J. Fish. Aquat. Sci., 65(7), 1321–1333, doi:10.1139/F08-047, 2008.

Willis, K., Cottier, F., Kwasniewski, S., Wold, A. and Falk-Petersen, S.: The influence of advection on zooplankton community composition in an Arctic fjord (Kongsfjorden, Svalbard), J. Mar. Syst., 61(1), 39–54, doi:https://doi.org/10.1016/j.jmarsys.2005.11.013, 2006.

Willis, K. J., Cottier, F. R. and Kwaśniewski, S.: Impact of warm water advection on the winter zooplankton community in an Arctic fjord, Polar Biol., 31(4), 475–481, doi:10.1007/s00300-007-0373-0, 2008.

Witman, J. D., Cusson, M., Archambault, P., Pershing, A. J. and Mieszkowska, N.: The relation between productivity and species diversity in temperate-arctic marine ecosystems, in Ecology., 2008.

Wood, T. M. and Gartner, J. W.: Use of acoustic backscatter and vertical velocity to estimate concentration and dynamics of suspended solids in Upper Klamath Lake, south-central Oregon: Implications for Aphanizomenon flos-aquae. [online] Available from: http://pubs.usgs.gov/sir/2010/5203/ (Accessed 27 June 2013), 2010.

https://doi.org/10.5194/os-2019-107
Preprint. Discussion started: 7 October 2019

Table 1. Abundance (ind. M^{-3}) and length (mm) of dominant zooplankton (>500 μm) in each bottle of the sediment trap at AN01, October 2016 to August 2017. Note: *T. libellula* juveniles and adults are presented separately for bottle 6, adult abundance and length are in parentheses.

Trap Bottle	Collection interval (dd/mm)	*Calanus glacialis*	*Limacina Helicina*	*Parasagitta elegans*	*Pseudocalanus* spp.	*Themisto libellula*
1 Abundance Length	4/10-8/11	58 3.2 ± 0.4	46 1.0 ± 0.5	412 23 ± 1.8	210 1.0 ± 0.2	8 8.3 ± 1.1
2 Abundance Length	8/11-13/12	22 3.3 ± 0.5	54 1.0 ± 0.3	114 23 ± 2.0	133 1.2 ± 0.2	21 20 ± 1.3
3 Abundance Length	13/12-17/01	14 3.5 ± 0.7	4 0.8 ± 0.04	129 24 ± 1.6	73 1.1 ± 0.2	28 21 ± 1.6
4 Abundance Length	17/01-21/02	5 3.4 ± 0.2	0	154 24 ± 2.0	38 1.0 ± 0.3	9 20 ± 1.7
5 Abundance Length	21/02-28/03	8 3.3 ± 0.4	0	77 24 ± 2.1	8 1.3 ± 0.0	5 27 ± 4.8
6 Abundance Length	28/03-02/05	3 3.4 ± 0.2	2 1.1 ± 0.1	56 25 ± 1.9	4 0.8 ± 0.2	191 (2) 2 (22)
7 Abundance Length	02/05-06/06	2 3.8 ± 0.4	13 1.2 ± 0.0	41 26 ± 3.0	4 0.9 ± 0.1	0
8 Abundance Length	06/06-11/07	0	21 1.6 ± 0.3	22 27 ± 1.9	1 1.3	0
9 Abundance Length	11/07-15/08	2 3.6 ± 0.1	5 1.5 ± 0.5	79 26 ± 2.5	5 1.1 ± 0.2	2 11 ± 3.5
10 Abundance Length	15/08-19/09	5 3.4 ± 0.8	61 1.1 ± 0.0	98 24 ± 2.2	8 1.1 ± 0.1	1 15

https://doi.org/10.5194/os-2019-107
Preprint. Discussion started: 7 October 2019

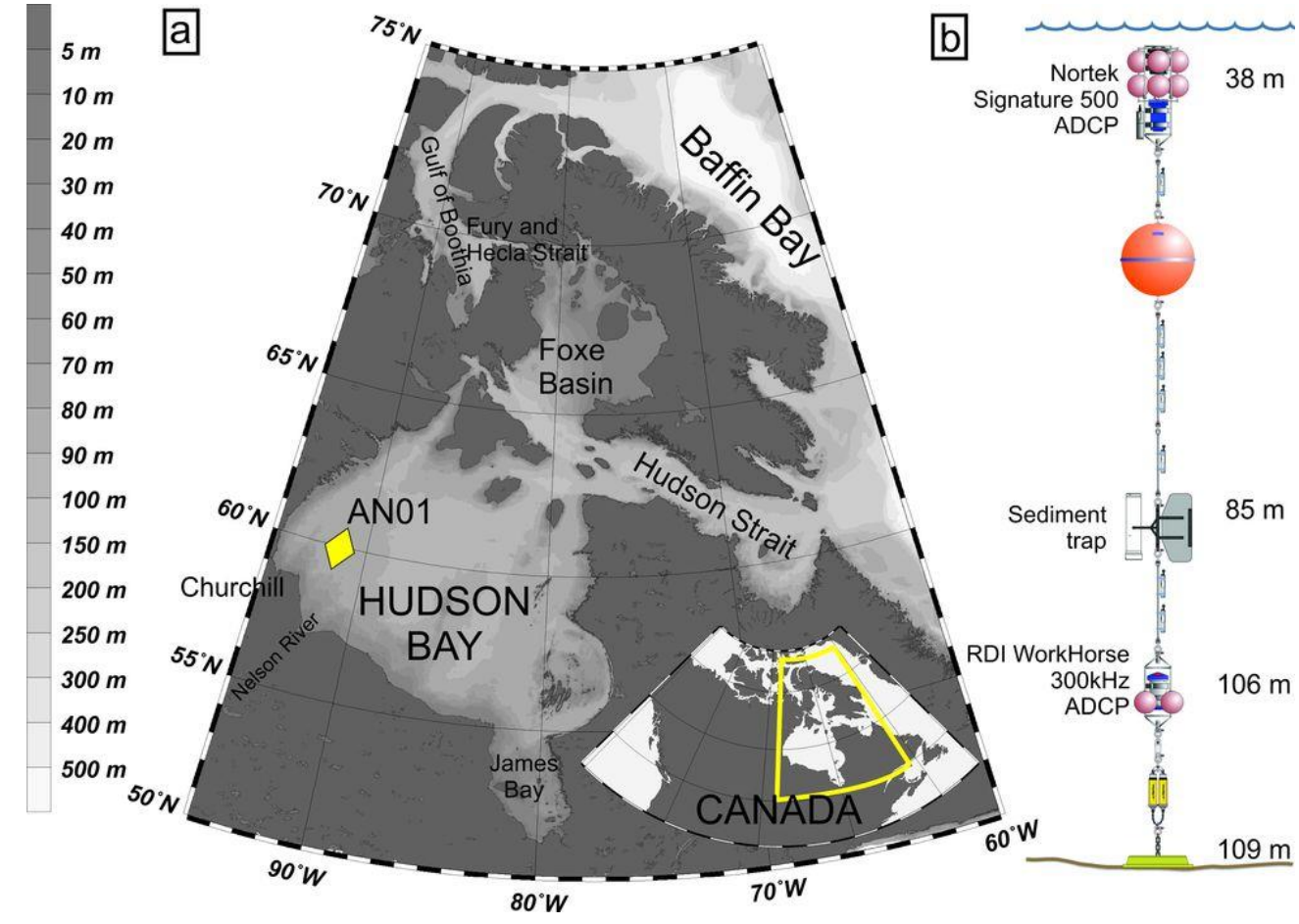

Figure 1. a) The bathymetric map of the Hudson Bay region and location of the mooring (AN01). The inset map shows Hudson Bay on the map of Canada. b) Schematic illustration of the mooring AN01 setup.

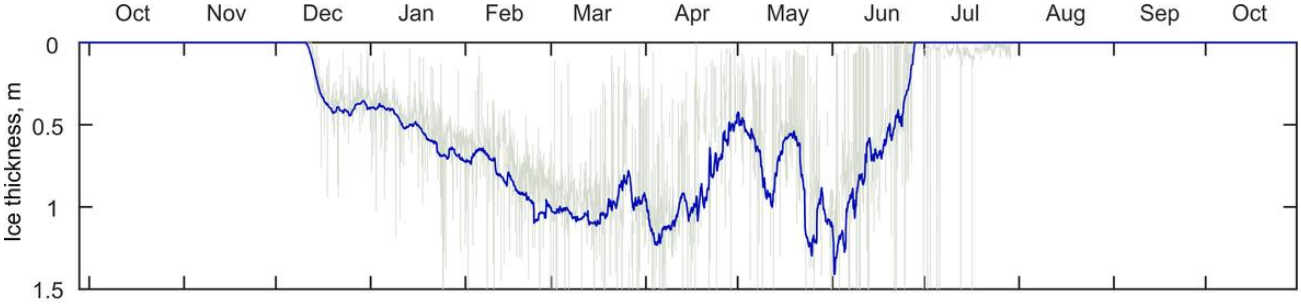

Figure 2. ADCP-measured ice thickness at the mooring location (AN01) during winter 2016-2017. Gray and blue lines represent the filtered and daily averaged ice thicknesses, respectively.

https://doi.org/10.5194/os-2019-107
Preprint. Discussion started: 7 October 2019

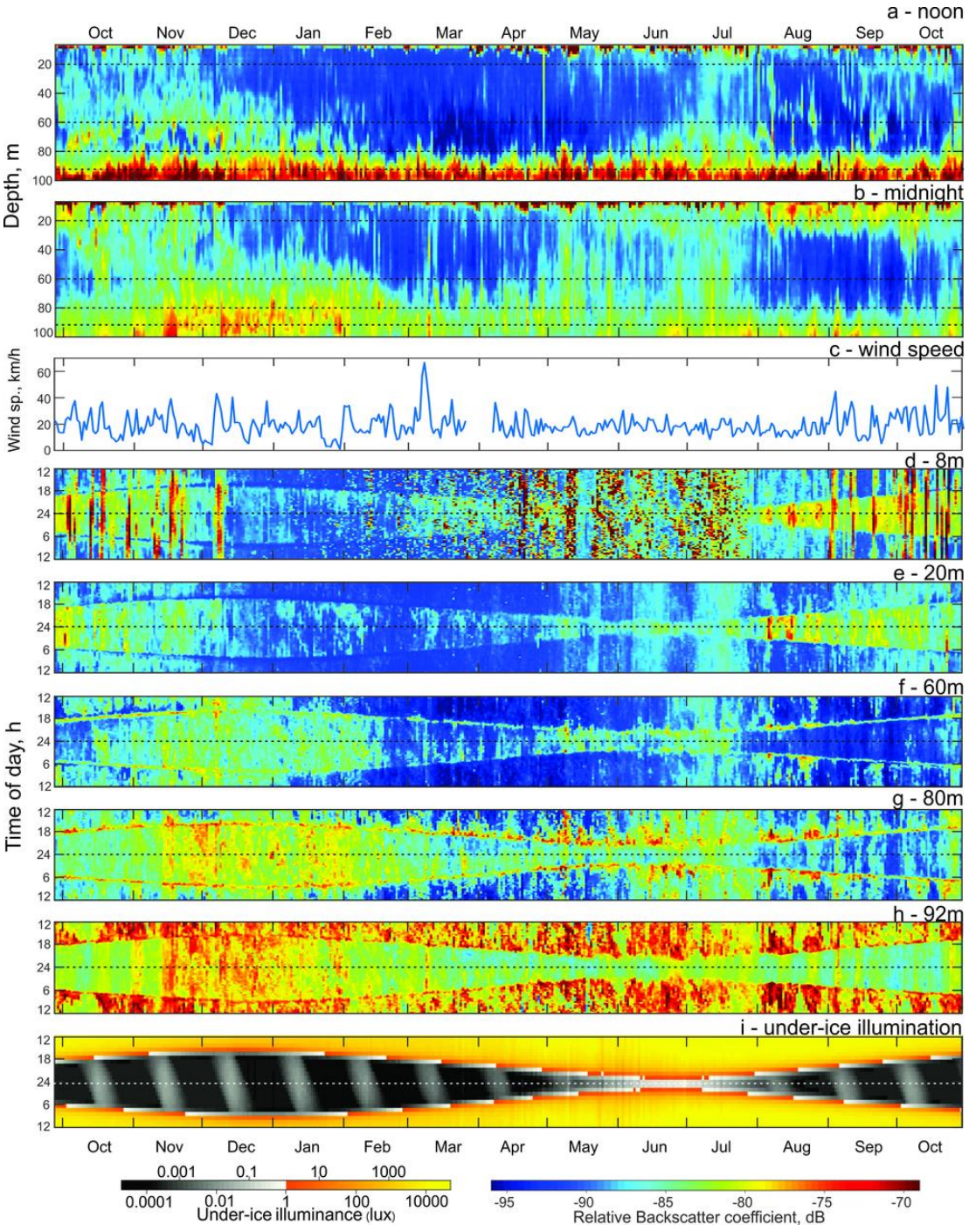

Figure 3. Time series (October 2016 to October 2017) of the (a) ADCP acoustic volume backscatter coefficient at noon and (b) at midnight, (c) daily mean wind speed measured at Churchill airport (YYQ), and (d-i) actograms of ADCP acoustic backscatter at five depth levels: (d) 8m, (e) 20 m, (f) 60 m, (g) 80 m and (h) 92 m and (i) modeled under-ice illuminance. Dashed horizontal lines represent the astronomical midnight. The diurnal signal is presented at the vertical axis, while the long-term changes in diurnal behaviour are presented along the horizontal axis.

https://doi.org/10.5194/os-2019-107
Preprint. Discussion started: 7 October 2019

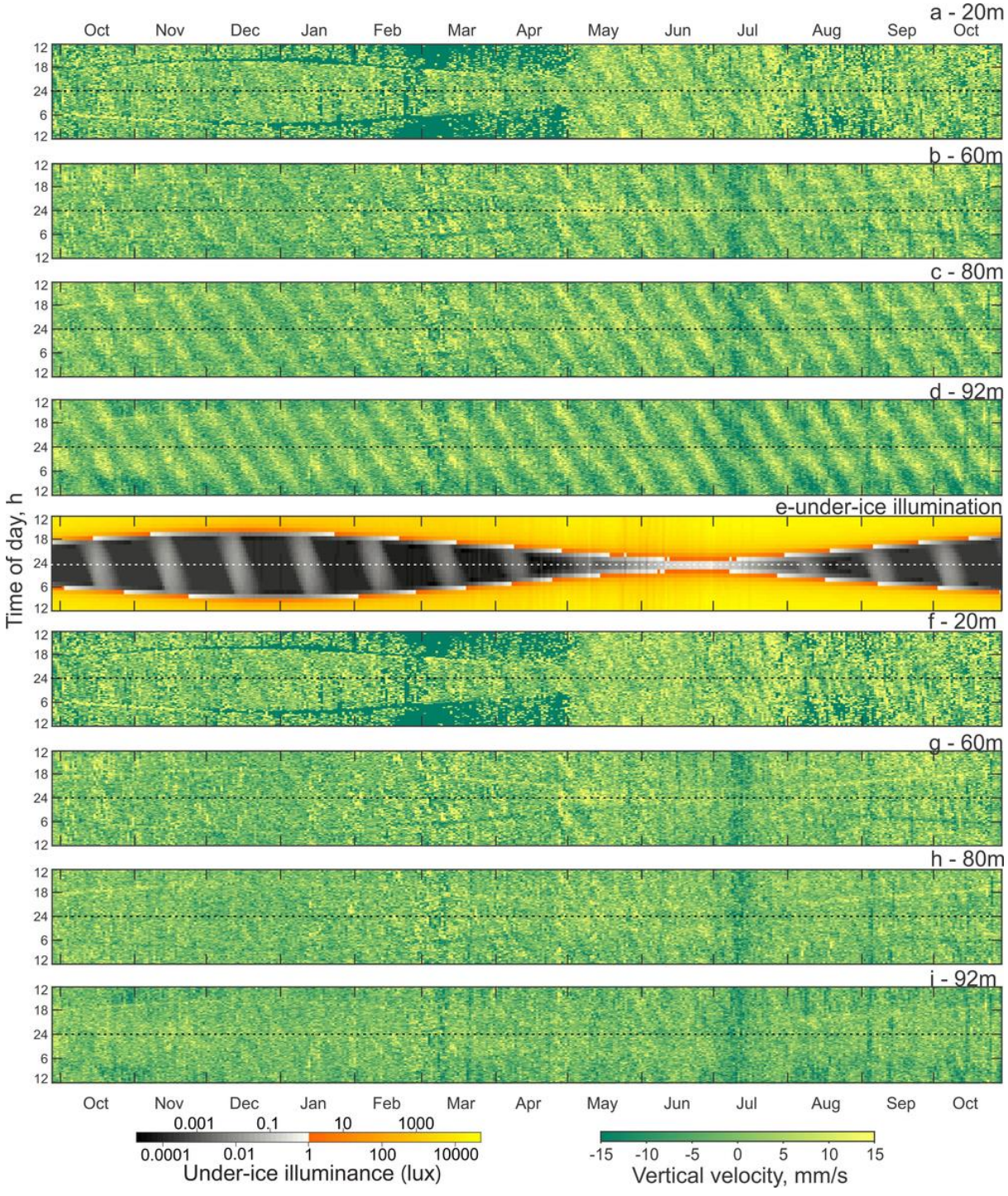

Figure 4. Actograms of (a-d) ADCP-measured vertical velocity (mm/s) at four depth levels: (a) 20 m, (b) 60 m, (c) 80 m and (d) 92 m, (e) modelled under-ice illuminance and (f-i) residual vertical velocity (mm/s, tidal signal subtracted) at four depth levels: (f) 20 m, (g) 60 m, (h) 80 m and (i) 92 m. Positive/negative values correspond to the upward/downward net flux. Dashed horizontal lines represent the astronomical midnight.

https://doi.org/10.5194/os-2019-107
Preprint. Discussion started: 7 October 2019

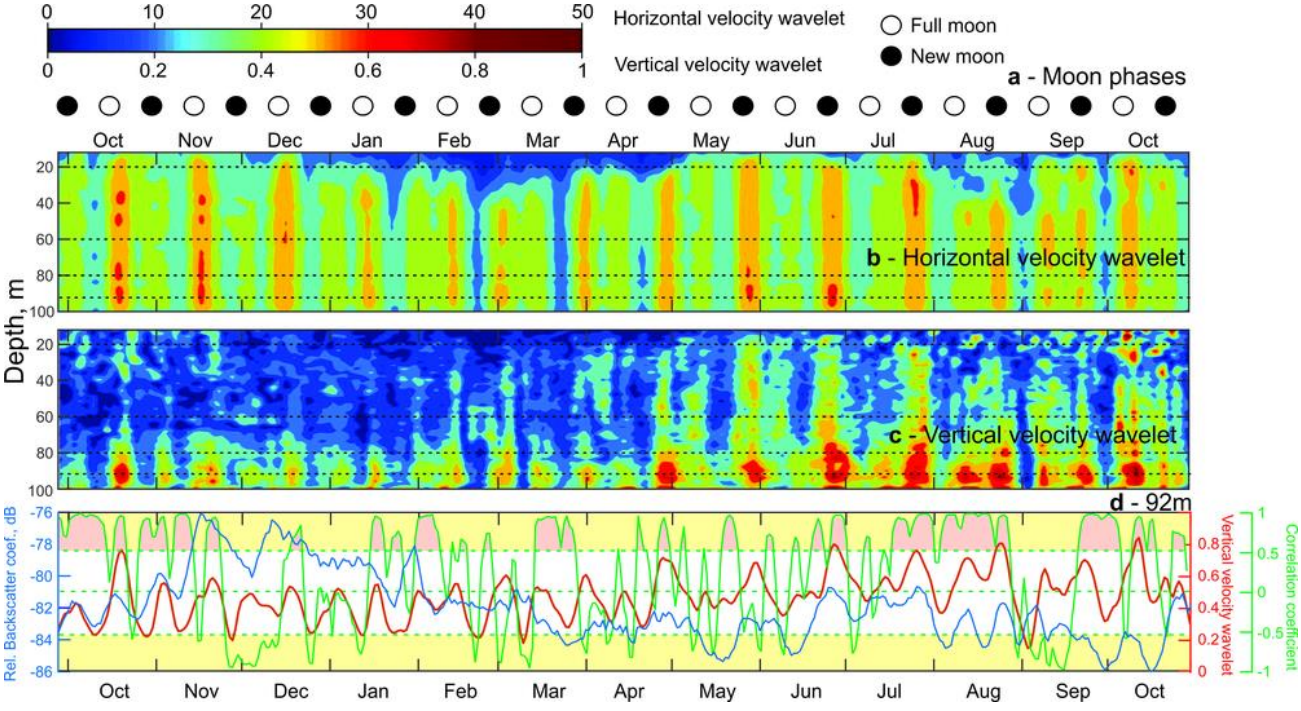

590 **Figure 5. Time series of (a) lunar phases for 2016 – 2017. ○ - Full moon. ● – New moon. (b) and (c) - the absolute value of wavelet power spectrum for the time series of horizontal velocity (b) and vertical velocity (c) computed for semi-diurnal frequency band (12 h) as a function of depth. (d) – the correlation coefficient (green line) between time series of VBS (blue line) and vertical velocity wavelet (red line) at 92 m depth. Yellow shading identifies the correlation coefficient levels exceeding ±0.53, which are statistically significant for the 95% confidence. Pink shading identifies the events when this statistically significant correlation was observed.**

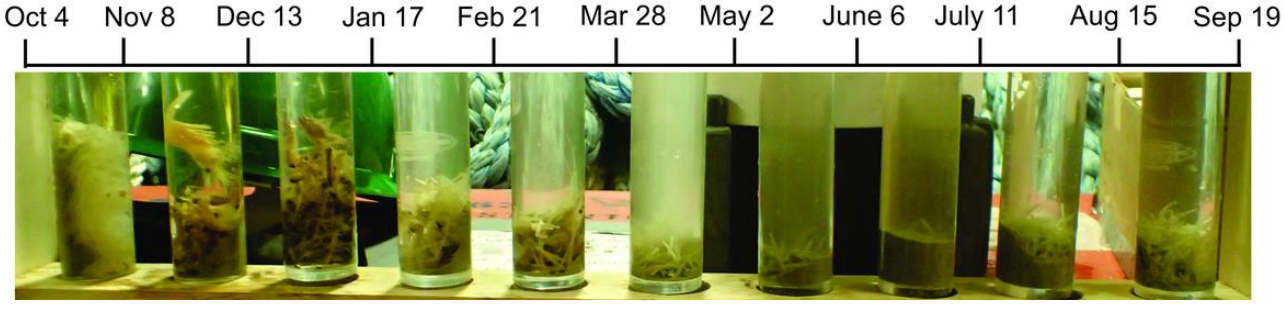

595 **Figure 6. Contents of the sediment trap for ten 35-day intervals.**

https://doi.org/10.5194/os-2019-107
Preprint. Discussion started: 7 October 2019

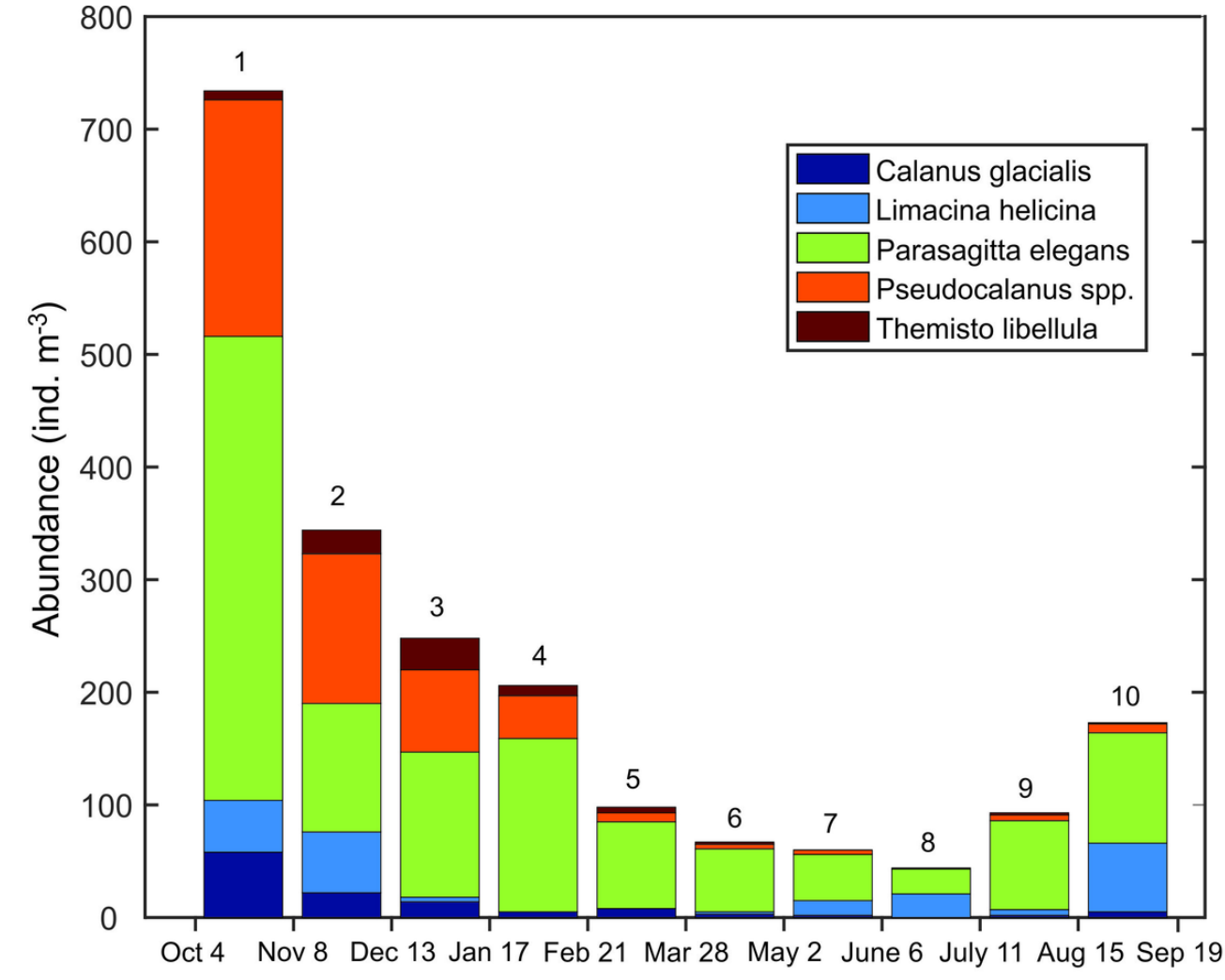

Figure 7. Abundance (ind. M^{-3}) of dominant zooplankton (>500 μm) in each bottle of the sediment trap at AN01, October 2016 to August 2017.